



# Linking roots, preferential flow, and soil moisture redistribution in deciduous and coniferous forest soils

Ziteng Luo<sup>1,2</sup> · Jianzhi Niu<sup>2,3</sup> · Shuqin He<sup>1</sup> · Linus Zhang<sup>4</sup> · Xiongwen Chen<sup>5,6</sup> · Bo Tan<sup>1</sup> · Di Wang<sup>2</sup> ·  
Ronny Berndtsson<sup>4</sup>

Received: 26 July 2022 / Accepted: 28 October 2022 / Published online: 18 November 2022  
© The Author(s), under exclusive licence to Springer-Verlag GmbH Germany, part of Springer Nature 2022

## Abstract

**Purpose** Soil moisture (i.e., the changes in the gravimetric soil water content) redistribution is closely linked with root distribution and preferential flow in soils. This study aimed at exploring the soil water content distribution in the presence of root-enhanced preferential flow in deciduous (*Quercus variabilis* BI.) and coniferous forests (*Platycladus orientalis* (L.)).

**Methods** Dual-tracer experiments (Brilliant Blue FCF and Bromide [Br<sup>-</sup>]) were conducted in both forests under large (40 mm) and extreme (70 mm) rainfall amount. The distribution of soil water contents was investigated in vertical soil profiles after dual-tracer experiments. Additionally, the correlations among soil water contents, root traits (diameter  $\leq$  5 mm), and preferential flow features (preferential flow paths and root-solute interaction) were analyzed.

**Results** Abundant root-induced soil moisture accumulation was found in the upper soil layer (0–20 cm), which was more apparent in deciduous forest than in coniferous forest. Preferential flow strongly influenced the variation distribution of soil water content. The greater degree of preferential flows was, the higher soil water content was. In both forests, the effect of root traits on soil water distribution was more evident under large rainfall amount as compared to extreme rainfall amount. In addition, positive significant correlation between root-solute interaction and soil water content was found at both sites.

**Conclusions** These results indicated that tree species with different roots distribution patterns enhance different degree of preferential flow, and have varied impacts on the soil moisture redistribution in forest soils. The effects of root traits on soil moisture are more apparent under lower rainfall amount.

**Keywords** Roots · Dual-tracer experiment · Preferential flow · Soil moisture · Forest

---

Responsible editor: Xiaoqi Zhou

---

✉ Jianzhi Niu  
nexk@bjfu.edu.cn

✉ Shuqin He  
angelhsq@163.com

<sup>1</sup> National Forestry and Grassland Administration Key Laboratory of Forest Resources Conservation and Ecological Safety on the Upper Reaches of the Yangtze River, Sichuan Province Key Laboratory of Ecological Forestry Engineering on the Upper Reaches of the Yangtze River, Soil and Water Conservation and Desertification Control Key Laboratory of Sichuan Province, College of Forestry, Sichuan Agricultural University, 211 Huimin Road, Chengdu, Sichuan 611130, China

<sup>2</sup> Key Laboratory of State Forestry Administration on Soil and Water Conservation, Beijing Engineering Research

Center of Soil and Water Conservation, Engineering Research Centre of Forestry Ecological Engineering, Ministry of Education, School of Soil and Water Conservation, Beijing Forestry University, Beijing 100083, China

<sup>3</sup> Beijing Collaborative Innovation Center for Eco-Environmental Improvement With Forestry and Fruit Trees, Beijing 102206, China

<sup>4</sup> Division of Water Resources Engineering & Centre for Advanced Middle Eastern Studies, Lund University, Box 118, Lund SE-221 00, Sweden

<sup>5</sup> Department of Biological and Environmental Sciences, Alabama A&M University, Normal, AL 35762, USA

<sup>6</sup> Jiyang College, Zhuji, Zhejiang 311800, China

## 1 Introduction

Preferential flow is one of the most prominent components of the hydrologic cycle. Different from uniform flow, preferential flow moves fast along macropores (e.g., root channels, earthworm caves, cracks) and bypasses the denser and less-permeable soil matrix in the vadose zone (Allaire et al. 2009; Backnäs et al. 2012; Beven and Germann 2013; Laine-Kaulio et al. 2015). As the sign of transport of water and solutes from homogeneous to heterogeneous research, many studies have found that preferential flow has critical impacts on the leaching and bioavailability of nutrients, reducing soil erosion and increasing groundwater recharge, soil fertility, vegetation growth, and forest productivity (Jiang et al. 2015; Keesstra et al. 2016; Legout et al. 2009; Luo et al. 2019a; Mei et al. 2018; Zuo et al. 2021).

As a key factor in the “vegetation-soil-hydrology” system, plant roots have a significant impact on soil water flow (Porporato et al. 2002; Rodríguez et al. 2018; Liu et al. 2019a). Living or decayed roots are the most important type of macropore channels in forest soils. Roots’ distribution patterns (Luo et al. 2019b), amount (Dusek et al. 2006; Jørgensen et al. 2002), size (Cui et al. 2019; Guo et al. 2020), states of life (Ghestem et al. 2011; Wu et al. 2021), and system types (Jiang et al. 2018; Liu et al. 2020) can influence the preferential flow processes (Helliwell et al. 2017; Schwärzel et al. 2012; Zhang et al. 2017). Well-connected root channels lead preferential flow transport, thus bypassing the main part of the soil matrix (Guo et al. 2019a). In general, the influence of roots on preferential flow is manifold. Extensive research has investigated the importance of root channels promoting high percolation into deeper soil layers (Cui et al. 2019; Guo et al. 2019a, 2020; Wu et al. 2021). However, recent studies suggested that root distribution patterns in soil layers can influence the preferential flow direction and impede the vertical flow transport (Luo et al. 2019b). Both vertical and lateral water flow along the root system can affect water redistribution and cause spatial heterogeneity of soil nutrients (Revelli and Ridolfi 2003; Wu et al. 2021). Higher root amounts, higher water flow, and solute transport rates were found in preferential flow paths as compared to soil matrix (Hendrickx and Flury 2001; Zhang et al. 2017). As the main site of water transport during infiltration process, preferential flow strongly affected the variability of soil water content (Mei et al. 2018; Sanders et al. 2012). The soil moisture redistribution in different directions result from soil water flow process can alter the water supply which is the vital for plant growth (Zhu et al. 2019). Many recent studies have highlighted that heterogeneous soil moisture redistribution controlled by preferential flow was expected to be linked

with soil functions like biogeochemical process (Bak et al. 2019; Franklin et al. 2021; Tecon and Or 2016; Young and Bengough 2018). Furthermore, soil water content is the key influence parameter in characterization and modeling of soil water flow (Dubus and Brown 2002; Guo et al. 2019b; Liu and Lin 2015; Sheng et al. 2014; Wang et al. 2022; Zhang et al. 2015). Therefore, there are vital interplays among root traits, preferential flow and variations in rhizosphere soil moisture.

Deciduous and coniferous trees with different root distributions can enhance diverse preferential flow patterns (Luo et al. 2019b). These two kinds of forests in northern China play an important role for increasing soil infiltration and conserving water, especially during rainy season (June–September) when high-intensive rainfall events are common (Liu et al. 2019b). Soil water from infiltrating rainfall is vital for these types of trees, and sustain plant growth (Liu et al. 2017). In forest soils, root-enhanced preferential flow was largely responsible for water percolation and solute migration during larger and high-intensive rainfall events (Luo et al. 2019a, b; Yan and Zhao 2016). Therefore, investigating the relationships among root, preferential flow, and soil water redistribution can enhance the comprehension of the governing preferential flows in forest systems, improve the understanding of the soil–plant–atmosphere continuum, and facilitate the management of water resources in forest soils. Several researchers have shown that the soil moisture content is positively related to various root structural traits of different root systems in grasslands (Huang et al. 2016, 2019; Liu et al. 2019a). However, not much research has so far focused on the relations between root, preferential flow, and soil water spatial distribution in forest soils.

In view of the above, this paper aimed to investigate the relations among soil water content distribution, roots traits, and preferential flow by using dual-tracer experiments in deciduous (*Quercus variabilis* BI.) and coniferous forests (*Platycladus orientalis* (L.) Franco) under different rainfall amounts (large and extreme rainfall amounts) in northern China. We aimed to determine (a) the redistribution patterns of soil water content in soil profiles at the presence of preferential flow in forest soils, and (b) the response of soil water content to root traits and preferential flow in deciduous and coniferous forests.

## 2 Materials and methods

### 2.1 Experiment sites

This study was carried out in the Jiufeng National Forest Park (40°03'54"N, 116°05'45"E) located northwest of Beijing, China, and occupying a total area of 16 km<sup>2</sup> with forest coverage rate of 96.4%. The research station is strongly

**Table 1** Soil physical properties in the 0–40 cm soil layer (mean  $\pm$  SE)

Forest type	Dominant tree species	Soil layer	ISWC (%)	BD (g/cm <sup>3</sup> )	TP (%)	Ks (mm/min)
DF	<i>Quercus variabilis</i> Bl.	0–10	10.65	1.32 $\pm$ 0.06	50.10 $\pm$ 2.44	1.32 $\pm$ 0.42
		10–20	8.31	1.38 $\pm$ 0.15	48.01 $\pm$ 5.54	1.22 $\pm$ 0.72
		20–30	8.22	1.42 $\pm$ 0.04	46.24 $\pm$ 1.68	0.62 $\pm$ 0.47
		30–40	10.75	1.37 $\pm$ 0.08	48.30 $\pm$ 3.20	0.34 $\pm$ 0.15
CF	<i>Platycladus orientalis</i> (L.)	0–10	12.73	1.21 $\pm$ 0.13	54.16 $\pm$ 4.93	2.47 $\pm$ 0.82
		10–20	14.10	1.24 $\pm$ 0.13	53.25 $\pm$ 4.76	1.52 $\pm$ 0.91
		20–30	12.47	1.23 $\pm$ 0.10	53.48 $\pm$ 3.61	2.38 $\pm$ 1.64
		30–40	12.57	1.18 $\pm$ 0.13	55.34 $\pm$ 4.92	1.99 $\pm$ 0.81

SE standard error of mean; DF deciduous forest; CF coniferous forest; ISWC initial soil water content; BD bulk density; TP total porosity; Ks soil saturated hydraulic conductivity

influenced by warm and temperate semi-humid to semi-arid continental monsoon climate. Annual average temperature is 12.5 °C, and the annual average precipitation is about 660 mm with 70% occurring during summer from June to September. The average age of existing forests in the study area is 55 years. The forests are mainly planted with *Platycladus orientalis* (L.), *Pinus tabulaeformis* Carr., *Quercus variabilis* Bl., and *Robinia pseudoacacia*. We selected two typical deciduous forests (DF) and coniferous forests (CF) sites dominated by either *Quercus variabilis* Bl. or *Platycladus orientalis* (L.) as study sites. At both sites, the soil texture is loam (Luo et al. 2019b). Dual-tracer experiments were performed in both sites. Brilliant Blue FCF has traits of vivid color, limited toxicity, and easy adsorption (Zhu et al. 2019). Additionally, bromide has high water-solubility, low background concentration, and nonreactive nature (Sheng

et al. 2014). Therefore, tracing experiments with these two kinds of tracers can describe the water and solute flow comprehensively (Schwen et al. 2014). For each site, the initial soil water content (ISWC) of one soil layer was measured by the mixed up 4 soil samples from the same soil layer (0–10, 10–20, 20–30, and 30–40 cm). Finally, these soil samples were dried at 105 °C for 24 h to obtain initial soil water content (ISWC) (Table 1). In each site, plot (130 cm × 130 cm) was divided into two same subplots (65 cm × 130 cm) to perform dual-tracer experiments under large (40 mm) and extreme (70 mm) rainfall application amounts. Totally, 93 L mixed solution (Brilliant Blue: 5 g/L and Br<sup>-</sup>: 10 g/L) was uniformly sprinkled onto each plot. After 24 h, the dyed soil profiles were obtained and photographed (Fig. 1). The detail procedures were described in Luo et al. (2019b). Near each plot, undisturbed soil cores (200 cm<sup>3</sup>) with four replicates at

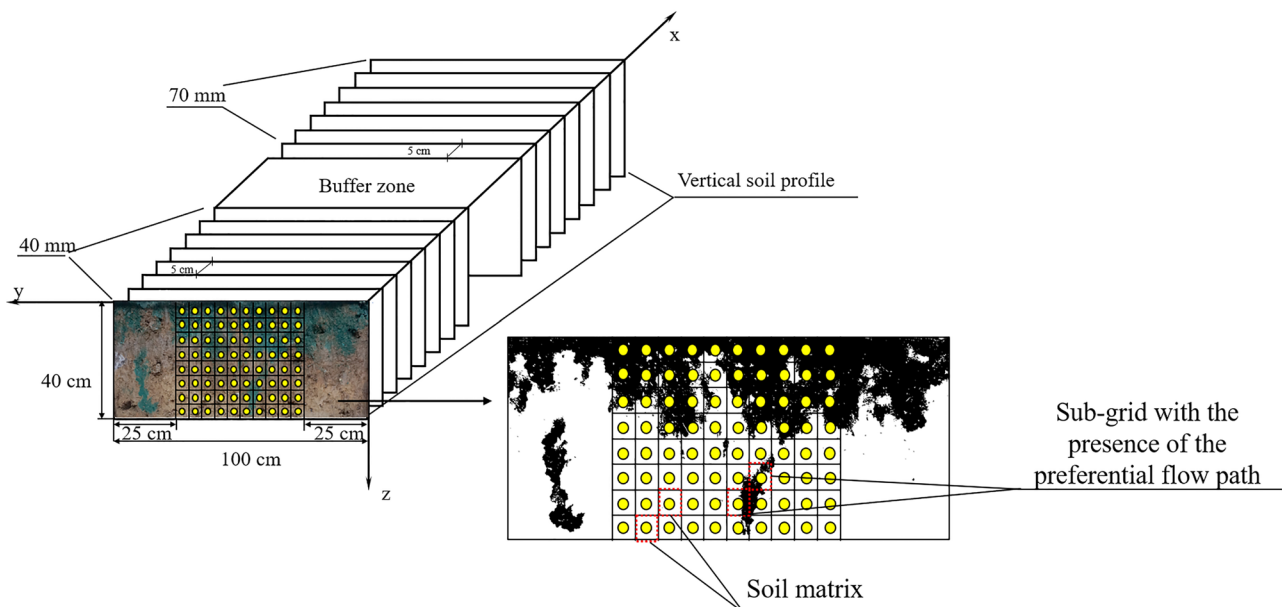


**Fig. 1** Schematic of soil sampling for vertical soil profiles at each experimental site

every 10 cm by ring knife were used to measuring soil saturated hydraulic conductivity ( $K_s$ ) (Mei et al. 2018). Intact soil cores of  $200 \text{ cm}^3$  with four replicates were collected at 0–10, 10–20, 20–30, and 30–40 cm to measure bulk density (BD) and total porosity (TP). Additionally, four replicates of undisturbed soil cores ( $200 \text{ cm}^3$ ) were collected by ring knife at every 10 cm in 0–40 cm soil layer to measure the root traits. Afterward, roots were sieved out and soaked in water carefully to remove attached soil particles (Wu et al. 2017). Finally, root samples (diameter  $\leq 5 \text{ mm}$ ) were scanned by EPSON Expression 1680 1.0, and analyzed by WinRHIZO (std 4800) (Luo et al. 2019a).

## 2.2 Soil sample collection for soil water content and root-solute interaction

After the dyed soil profiles' images were taken, the distribution of soil water content in vertical soil profiles was investigated using a gridded frame (50 cm by 40 cm) that put at 25 cm from the left and right edges of each soil vertical profile (Fig. 1). The maximum depth of vertical excavation was 40 cm, which limited by the maximum vertical dye-stained depth and the location of bedrock. Approximately 70 g soil were collected from each sub-grid (5 cm  $\times$  5 cm). For each sub-grid area (5 cm  $\times$  5 cm) that had a dye-stained area  $> 0$  defined as a section with presence of preferential flow. Sections that were unstained by dye tracer were regarded as soil matrix without preferential flow (Zhang et al. 2017) (Fig. 1). In total, 1280 soil samples were obtained from the 16 soil profiles at each site. All these samples were dried at 105 °C for 24 h to estimate the spatial of gravimetric soil water content (SWC). Then, these samples were used to measure solute content ( $\text{Br}^-$ ) and calculate RSI (Schwen et al. 2014; Luo et al. 2019b).

$$RSI = RA(C - C_{min})/(C_{max} - C_{min}) \quad (1)$$

where  $RA$  is the root abundance (number/dm $^2$ );  $C$  is the  $\text{Br}^-$  concentration (mg/(kg soil)) of soil samples collected in each 5  $\times$  5 cm grid (Fig. 1).  $C_{min}$  and  $C_{max}$  are maximum and minimum  $\text{Br}^-$  concentration collected in each dyed soil profiles, respectively. The detailed measurement procedure of concentration of  $\text{Br}^-$  and  $RA$  was described by Luo et al. (2019a, b).

## 2.3 Indicators of preferential flow paths

The detailed procedure of images' (dyed vertical soil profiles) analysis processes was described by Luo et al. (2019b). The preferential flow paths' uniform percolation depth (UniFr, cm), preferential flow fraction (PF-fr, %), length index (LI, %), and dye coverage (DC, %) were calculated following the study of Mei et al. (2018). Soils with a high

degree of preferential flow will have a higher LI and PF-fr, while lower UniFr (Bargués Tobella et al. 2014). Additionally, CV (coefficient of variation of DC) and FD (fractal dimension) were quoted from Wu et al. (2014) and Dai et al. (2020).

### 2.3.1 Coefficient of variation of DC

Coefficient of variation (CV) was used to caculated the DC differences (induced by preferential flow) between dyed region and undyed soil sections. Soils with a high degree of preferential flow will have a lower CV (Wu et al. 2014).

$$CV = \sqrt{(1/(n-1)) \sum_{i=1}^n (DC_i - \overline{DC})^2} / 1/n \sum_{i=1}^n DC_i \quad (2)$$

where  $n$  is the number of soil layer, and  $DC_i$  is the dye coverage of layer  $i$  (%).  $\overline{DC}$  is the average dye coverage for the entire soil profile (%).

### 2.3.2 Fractal dimension

Fractal dimension (FD) represents the complicated degree of fractal particle, which is the most important concept in fractal theory, calculated using Eq. (3) (Dai et al. 2020).

$$FD = \lim_{\varepsilon \rightarrow 0} \log N(\varepsilon) / \log (1/\varepsilon) \quad (3)$$

where  $\varepsilon$  and  $N(\varepsilon)$  are the length of one side of the small cube and the number of such cube, respectively. These cube just enough to cover the measured fractal particle. For dyed vertical soil profiles, the larger the FD, the more complicated the preferential flow paths, and the stronger hydrological connectivity (Dai et al. 2020).

## 2.4 Statistical analyses

Normal distributions of the experimental datasets were assessed with the Shapiro–Wilk test. The differences of roots and soil water content (SWC) features among the various soil layers were analyzed. If datasets met or transformed into normal distribution, they were analyzed by One-way ANOVA followed by a Turkey test. Otherwise, the Kruskal–Wallis test was used to assess. All statistical procedures were performed with a p-value of 0.05. The difference between root traits at the DF and CF sites, preferential flow indicators at the DF and CF sites, SWC at DF and CF sites were assessed. If the experimental datasets fit or transformed into the normal distribution, the independent-sample  $t$  test ( $P < 0.05$ ) were used to assess. Otherwise, a nonparametric Mann–Whitney U test was used with the least significant difference of  $P < 0.05$ . Correlations between preferential flow and soil water content were assessed using Pearson

correlation analysis. Spearman's correlation coefficients analysis was used to investigate the correlations between root traits and SWC, and among root-solute interaction (RSI) and SWC. Significant correction coefficients were tested at  $P < 0.05$ ,  $P < 0.01$ . All statistical analyses were performed using SPSS 25.0 (IBM, USA) and all the figures were created by Origin Pro 2021b software.

### 3 Results

#### 3.1 Distribution of root traits

The features of root traits were presented in Table 2. Generally, all root traits showed a consistent trend with increasing soil depth. Total RA, RLD, RSD, and RVD were high at the shallow soil layer (0–10 cm), and reached their minimum values (3.31 number/dm<sup>2</sup>, 8.70 mm/cm<sup>3</sup>, 9.66 mm<sup>2</sup>/cm<sup>3</sup>, and 2.55 mm<sup>3</sup>/cm<sup>3</sup>) at 30–40 cm soil layer. The mean RA of 0–10 cm was significantly larger than 10–40 cm in DF site ( $P < 0.05$ ). In the 0–20 cm, the mean RLD (44.60 mm/cm<sup>3</sup>) of DF was significantly larger than that of CF ( $P < 0.05$ ). However, in 20–40 cm, the mean RA (4.24 /dm<sup>2</sup>) and RSD (12.98 mm<sup>2</sup>/cm<sup>3</sup>) of DF were significantly lower than that of CF ( $P < 0.05$ ). Root traits were also various among different root diameter classes. In both sites, the RLD and RSD decreased as the root diameter classes increases evidently. For RVD, the value of  $d \leq 2$  mm was significantly larger than that of  $2 < d \leq 5$  mm ( $P < 0.05$ ).

#### 3.2 Characteristics of preferential flow paths

Indices of preferential flow paths in DF and CF under large and extreme rainfall amounts are shown in Fig. 2. The features of preferential flow paths indicated a difference between DF and CF under large (40 mm) and extreme (70 mm) rainfall amounts. For the DF site, the mean UniFr, PF-fr, LI, FD, and DC under extreme rainfall were higher than that of large rainfall ( $P > 0.05$ ). Meanwhile, the mean CV was  $1.01 \pm 0.11\%$  for larger rainfall, which was significantly larger than that for extreme rainfall ( $0.86 \pm 0.08\%$ ) ( $P < 0.05$ ). At the CF site, the DC under large rainfall was lower than that of under extreme rainfall ( $P > 0.05$ ). There was no significant difference between the mean PF-fr for the large and extreme rainfall amount ( $P > 0.05$ ). Additionally, the mean UniFr, LI, and FD under extreme rainfall was significantly higher than that of under large rainfall ( $P < 0.05$ ). However, the mean CV was significantly higher under large rainfall as compared to the extreme rainfall amount ( $P < 0.05$ ).

For the large rainfall amount, the mean CV and FD of DF showed no significant difference with those of CF ( $P > 0.05$ ). Meanwhile, the mean PF-fr of DF was

Forest type	Dominant tree species	Soil layer (cm)	RA (number/dm <sup>2</sup> )	RLD (mm/cm <sup>3</sup> )	RSD (mm <sup>2</sup> /cm <sup>3</sup> )				RVD (mm <sup>3</sup> /cm <sup>3</sup> )			
					$d \leq 1$ mm		$1 < d \leq 2$ mm		$2 < d \leq 5$ mm		$d \leq 1$ mm	
					$d \leq 1$ mm	$1 < d \leq 2$ mm	$2 < d \leq 5$ mm	$d \leq 1$ mm	$1 < d \leq 2$ mm	$2 < d \leq 5$ mm	$d \leq 1$ mm	$1 < d \leq 2$ mm
DF	<i>Quercus variabilis</i> Bl	0–10	10.63 $\pm$ 3.11a	56.08 $\pm$ 17.85a	2.20 $\pm$ 0.52a	0.67 $\pm$ 0.57a	38.91 $\pm$ 5.93a	9.56 $\pm$ 2.31a	5.80 $\pm$ 5.48a	3.47 $\pm$ 0.49a	3.43 $\pm$ 0.85a	5.60 $\pm$ 7.17a
		10–20	7.97 $\pm$ 3.08b	29.10 $\pm$ 14.14ab	0.99 $\pm$ 0.41b	0.18 $\pm$ 0.16a	18.77 $\pm$ 8.56b	4.14 $\pm$ 1.79b	1.55 $\pm$ 1.39a	1.69 $\pm$ 0.71b	1.43 $\pm$ 0.66b	1.11 $\pm$ 0.98ab
		20–30	5.18 $\pm$ 2.45c	15.46 $\pm$ 3.97ab	0.80 $\pm$ 0.29b	0.30 $\pm$ 0.15a	9.96 $\pm$ 2.30bc	3.62 $\pm$ 1.30b	2.74 $\pm$ 1.56a	0.91 $\pm$ 0.24bc	1.35 $\pm$ 0.48b	2.13 $\pm$ 1.50ab
	<i>Platycladus orientalis</i> (L.) Franco	30–40	3.31 $\pm$ 2.08d	7.92 $\pm$ 2.76b	0.61 $\pm$ 0.57b	0.16 $\pm$ 0.31a	5.59 $\pm$ 2.36c	2.65 $\pm$ 2.52b	1.42 $\pm$ 2.79a	0.54 $\pm$ 0.30c	0.94 $\pm$ 0.93b	1.06 $\pm$ 2.10b
		10–20	9.63 $\pm$ 3.15a	39.31 $\pm$ 6.75a	1.96 $\pm$ 0.63a	0.33 $\pm$ 0.19a	36.05 $\pm$ 8.19a	8.19 $\pm$ 2.73a	2.71 $\pm$ 1.56a	4.00 $\pm$ 1.01a	2.82 $\pm$ 0.99a	1.84 $\pm$ 1.05a
		20–30	8.76 $\pm$ 2.46a	21.37 $\pm$ 7.13b	1.67 $\pm$ 0.25ab	0.32 $\pm$ 0.14a	19.03 $\pm$ 6.95b	6.92 $\pm$ 1.09ab	2.71 $\pm$ 1.00a	2.21 $\pm$ 0.81b	2.37 $\pm$ 0.41ab	1.92 $\pm$ 0.67a
		30–40	6.14 $\pm$ 2.21b	15.81 $\pm$ 7.50b	2.21 $\pm$ 0.51ab	0.44 $\pm$ 0.20a	13.82 $\pm$ 5.01b	9.70 $\pm$ 2.40ab	3.56 $\pm$ 1.71a	1.65 $\pm$ 0.60b	3.52 $\pm$ 0.94ab	2.42 $\pm$ 1.33 a
		40–50	3.81 $\pm$ 1.72c	15.02 $\pm$ 8.22b	0.96 $\pm$ 0.48b	0.14 $\pm$ 0.24a	10.46 $\pm$ 3.09b	4.10 $\pm$ 2.28b	1.08 $\pm$ 1.83a	1.14 $\pm$ 0.30b	1.46 $\pm$ 0.91b	0.66 $\pm$ 1.15a

SE standard error of mean; DF: deciduous forest, CF: coniferous forest, RA root abundance, RLD root length density, RSD root surface density, RVD root volume density. Different lowercase letters represent significant differences between different soil layers in each site ( $P < 0.05$ )

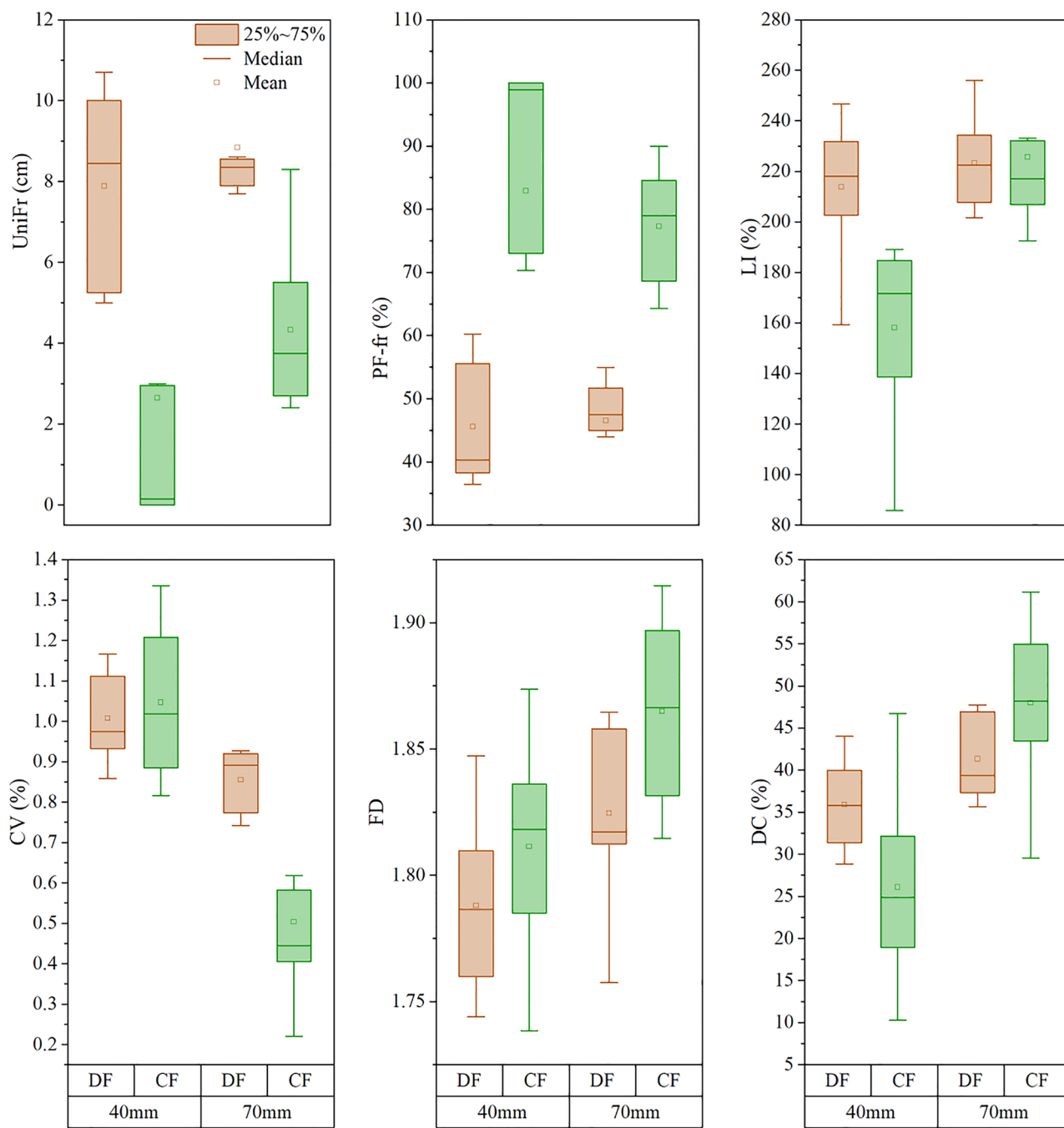


**Fig. 2** Boxplots (median, mean, first, and third quartile;  $n=8$ ) of preferential flow paths' indicates in deciduous (DF) and coniferous (CF) forest soils; DF and CF are deciduous and coniferous forests, respectively; UniFr, uniform percolation depth; PF-fr, preferential flow fraction; LI, length index; CV, coefficient of variation of DC; FD, fractal dimension; DC, dye coverage

tively; UniFr, uniform percolation depth; PF-fr, preferential flow fraction; LI, length index; CV, coefficient of variation of DC; FD, fractal dimension; DC, dye coverage

significantly lower as compared with CF ( $P < 0.05$ ). The mean UniFr of DF was  $7.89 \pm 2.39$  cm, which was significantly larger than that of CF ( $2.65 \pm 5.16$  cm) ( $P < 0.05$ ). Additionally, the mean LI and DC of DF was significantly larger than those of CF ( $P < 0.05$ ). For the extreme rainfall amount, the mean UniFr and CV of DF were

significantly larger than those of CF ( $P < 0.05$ ). However, the mean PF-fr and FD of DF were significantly lower as compared with those of CF ( $P < 0.05$ ). The mean LI ( $225.66 \pm 33.21\%$ ) and DC ( $48.00 \pm 10.16\%$ ) of CF was larger than those of DF, but difference was not significant ( $P > 0.05$ ).

### 3.3 Observed SWC (soil water content) distribution

The distribution of SWC along soil profiles in DF and CF under large (40 mm) and extreme (70 mm) rainfall amounts were shown in Fig. 3. At both sites, the SWC decreased with increasing depth, and the average SWC in the soil layer of 0–20 cm was significantly higher than that of 20–40 cm ( $P < 0.05$ ). This trend was more apparent at the DF site as compared with CF. At the DF site, mean SWC under extreme rainfall in 0–10, 10–20, 20–30, and 30–40 cm was 1.03, 1.04, 1.06, and 1.45 times mean SWC of each same soil layer for the large rainfall. Whereas the mean SWC was higher at the CF site under extreme rainfall as compared to that of the large rainfall for 0–40 cm ( $P < 0.05$ ).

Different SWC distribution patterns between  $DC > 0$  section (section with the presence of preferential flow) and  $DC = 0$  region (soil matrix) were observed (Fig. 4). The white regions in Fig. 4 indicated that there was no sample collected in  $DC > 0$  or  $DC = 0$  regions. For  $DC > 0$  sections, the small SWC areas are accumulated at 30–40 cm soil depth. For  $DC = 0$  sections, a large section with small SWC extends in the upper 0–10 cm soil layer. At the DF site, there was no significant difference of  $SWC_{DC>0}$  between large and extreme rainfall at 0–20 cm soil depth ( $P > 0.05$ ). With respect to deeper soil layers (20–40 cm), the  $SWC_{DC>0}$  under extreme rainfall was significantly higher than that of large rainfall ( $P < 0.05$ ). Meanwhile, the  $SWC_{DC=0}$  under extreme rainfall was about 24% larger than that of large rainfall, and there was a significant difference for  $SWC_{DC=0}$  between the

two kinds of rainfall for the 0–40 cm soil depth ( $P < 0.05$ ). For the CF site,  $SWC_{DC>0}$  under extreme rainfall was significantly higher than that of large rainfall for 0–40 cm soil depth ( $P < 0.05$ ). Moreover, a significant difference in  $SWC_{DC=0}$  was observed between the large and extreme rainfall for the same soil depth ( $P < 0.05$ ). In general, the proportion of  $SWC_{DC>0}$  above  $SWC_{DC=0}$  ranged from 76.19 to 95.23% at both sites under both rainfall amount types.

The difference between SWC in the two sections with  $DC > 0$  and  $DC = 0$  and initial soil water content (ISWC) is presented in Fig. 5. At both sites, SWC ( $SWC_{DC>0}$  or  $SWC_{DC=0}$ ) can be both larger or less than the ISWC after tracer experiments (under extreme or large rainfall amounts) (Fig. 5a). The proportion of SWC ( $SWC_{DC>0}$  or  $SWC_{DC=0}$ ) larger than ISWC decreased with soil depth for both sites. This phenomenon was more obvious at the DF site. Compared to DF, the proportion of  $SWC_{DC>0}$  larger than ISWC was higher at the CF site. Generally, the increase (as compared to ISWC) of SWC in  $DC > 0$  sections is greater than that in the  $DC = 0$  region after the dye experiment (under extreme or large rainfall amounts) (Fig. 5b).

### 3.4 Relations among roots, preferential flow, and SWC

#### 3.4.1 Relations between SWC and root traits

The correlations between root traits and SWC were shown in Table 3. For large rainfall amount, SWC had an extremely significant positive relationships with RA

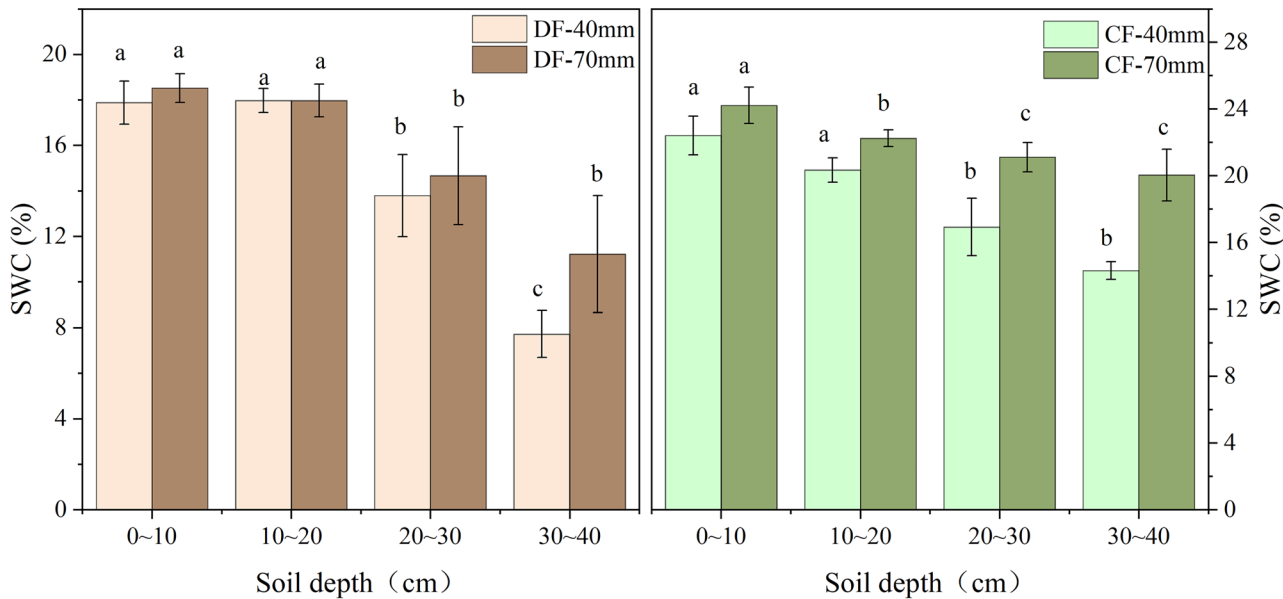


**Fig. 3** Features of soil water content in soil profiles along soil depth in typical forest soils; DF-40 and CF-40 mm were sampled for large rainfall amount (40 mm). DF-70 and CF-70 mm were sampled for extreme rainfall amount (70 mm). DF, deciduous forest; CF, conifer-

ous forest; SWC, soil water content. Lowercase letters represent significant difference among different soil layers under the same rainfall amount ( $P < 0.05$ )

( $P < 0.01$ ). In addition, SWC only extremely positively correlated with the RLD, RSD, and RVD of  $d \leq 1$  mm ( $P < 0.01$ ). For extreme rainfall amount, there was no significant correlations observed between SWC and RA ( $P > 0.05$ ). Besides, a positive relationship was noticed between SWC and RVD of  $d \leq 2$  mm ( $P < 0.05$ ).

### 3.4.2 Relations between SWC and preferential flow paths

At both sites, partial preferential flow indices presented significant correlation with SWC (Fig. 6). For the DF site, CV and DC showed significant negative and positive correlation with SWC, respectively ( $P < 0.05$ ). FD and SWC was positively significantly correlated ( $P < 0.01$ ). At the CF site, the FD, DC and LI were positively correlated with SWC ( $P < 0.01$ ). The CV was negatively significantly correlated with SWC ( $P < 0.01$ ).

**Fig. 4** Mean soil water content in different sections of typical forest soil profiles; DF and CF are deciduous and coniferous forests, respectively; DF-40 and CF-40 mm are for large rainfall amount (40 mm). DF-70 and CF-70 mm are for extreme rainfall amount (70 mm); SWC, soil water content. The white region indicate that there was no sample collected in DC > 0 or DC = 0 sections

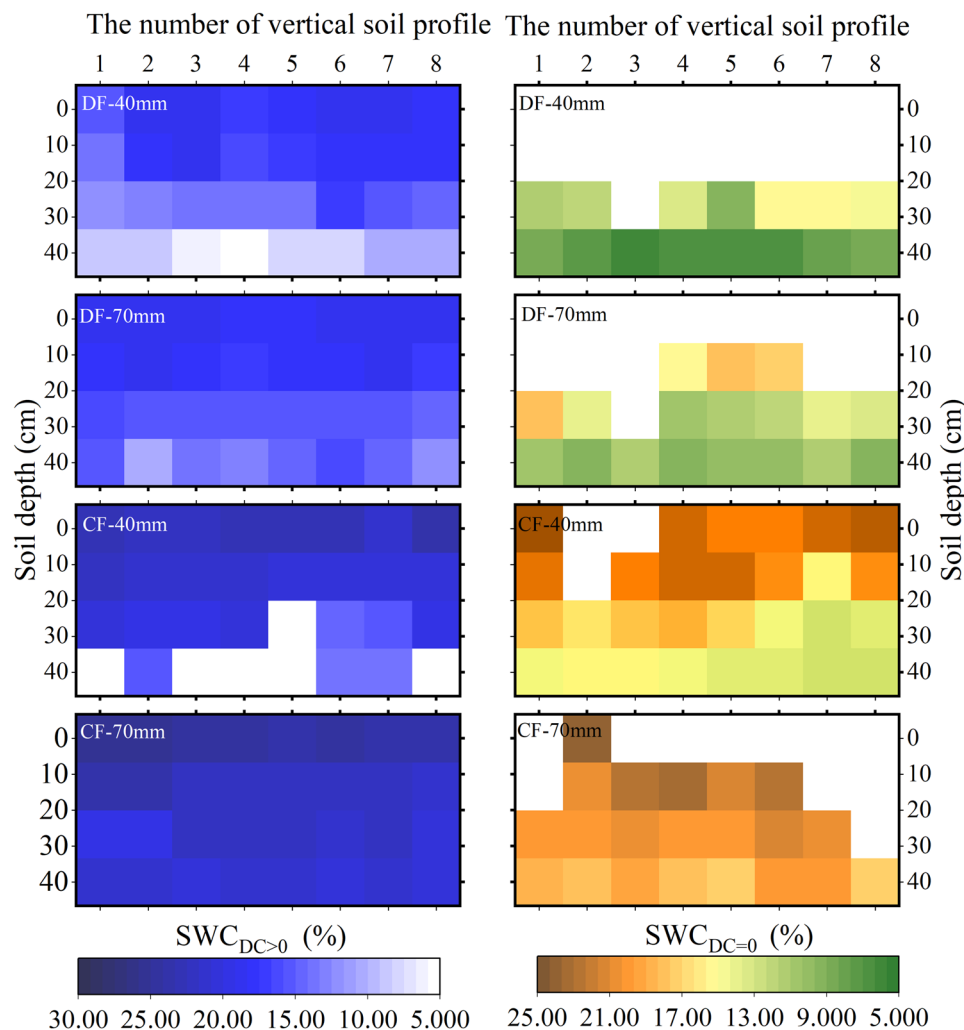
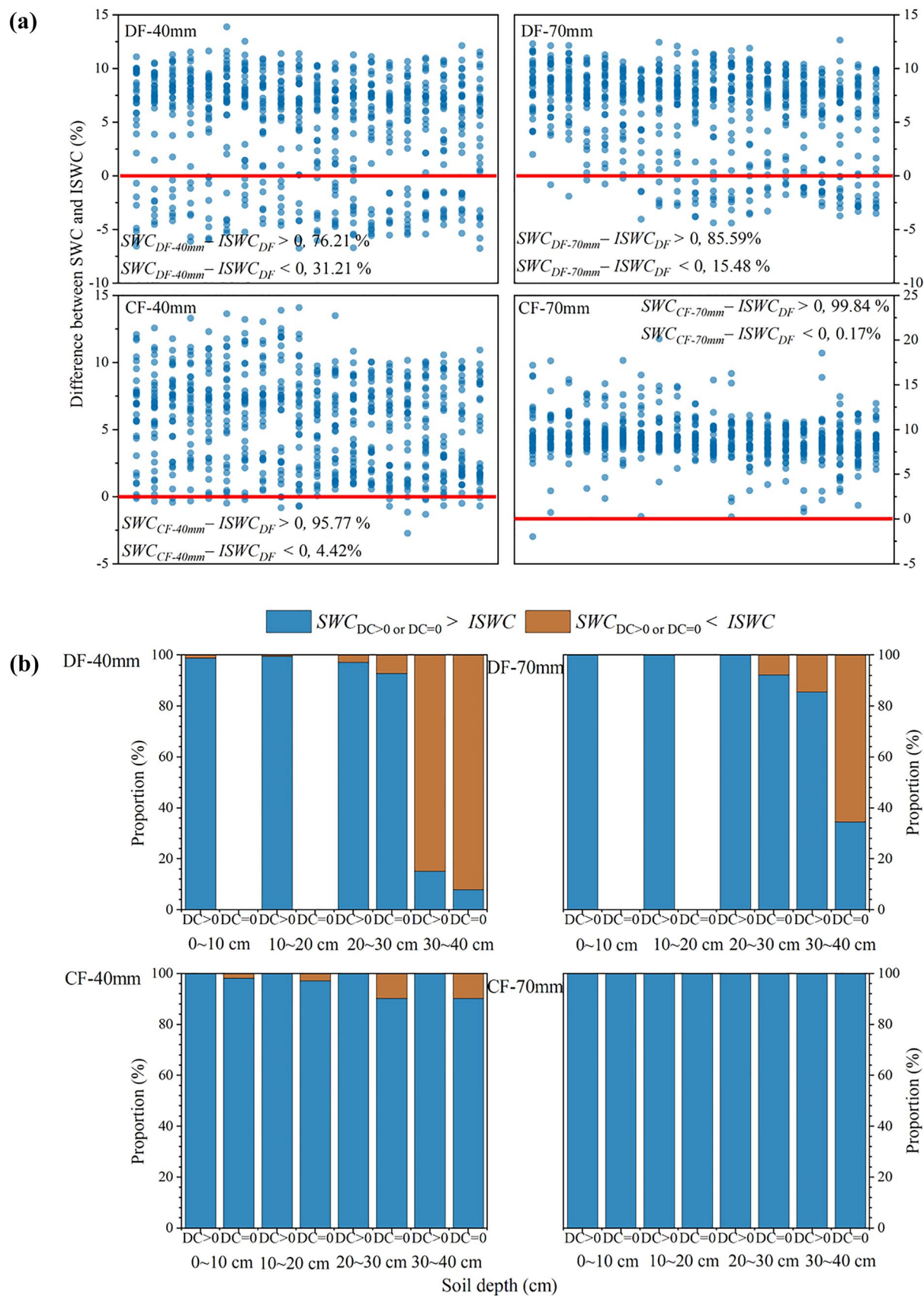


**Fig. 5** Comparison of oil water content in soil profiles and initial soil water content in typical forest soils; **a** comparison for whole soil profiles, and **b** comparison for different sections (DC > 0 and DC = 0); DF-40 and CF-40 mm are for large rainfall amount (40 mm). DF-70 and CF-70 mm are for extreme rainfall amount (70 mm). DF, deciduous forest; CF, coniferous forest; DC, dye coverage (%)

### 3.4.3 Relations between SWC and RSI (root solute interaction)

The correlation analyses showed that the RSI was positively correlated with SWC at both sites for both large and extreme rainfall amounts ( $P < 0.01$ ) (Fig. 7). The correlation coefficients between the RSI and SWC ranged between 0.371 and 0.566 ( $P < 0.01$ ). When RSI = 0, the SWC ranged from 12.69 to 21.34% at both sites, which was 1.14 and 1.07 times lower than that RSI > 0 in DF and CF, respectively.



## 4 Discussion

This study highlighted that SWC redistribution is closely linked with root distribution and preferential flow patterns (Table 2 and 3, Figs. 2–7). The degree of preferential flow and hydrological connectivity were stronger in CF than DF, especially during extreme rainfall (Fig. 2). This result is consistent with the results of our previous studies, which showed that the spatial variability of preferential flow paths is higher in CF soils as compared to DF soils (Luo et al. 2019b). The accumulated root distribution pattern in DF shallow soil layers impeded the vertical transport. However, better connected root channels in CF could induce higher degree of preferential flow as compared to DF soils (Table 2 and Fig. 2). When the rainfall increased from large to extreme, water and solute in CF soils can transport through entire soil profile and migrate into deeper soil layer than DF (Fig. 2). Meantime, the results of this study indicate that SWC decreased with the increase of soil depth in both sites (Fig. 3). Our findings are consistent with the results of Zuo et al. (2021) who stated that the soil moisture (soil volumetric water content) accumulated in shallow soil layers in *A. splendens* planting area. In forest, root can generate preferential flow path and remain for decades (Beven and Germann 2013). This kind of channels lead water and solute bypassing most of soil matrix (Backnäs et al. 2012; Laine-Kaulio et al. 2015). In both sites, all the root traits (RA, RLD, RSD, and RVD) decreased with soil depth evidently (Table 2), which concur with the study of Zhang et al. (2017). More than half of total roots were found in shallow soil layer (0–20 cm) (Table 2), which was in agreement with those studies of Ni et al. (2015) and Raizada et al. (2013). Thus, high SWC in shallow soil layer could be attributed to its root-induced well-structural macropore networks. In both sites, the area of preferential flow path was decreased along soil depth (Luo et al. 2019b). Macropores formed by biological activity (i.e., earth worm and roots) decreased along soil depth in forest soils (Meng et al. 2017). Therefore, the decrease of the interconnected macropore is an important reason for the decrease of SWC in the deep soil layer (Fig. 3). Additionally, soil water can transport from preferential flow path into soil matrix and stored for root absorption (de Lima et al. 2022; Gao et al. 2021; Lepore et al. 2009; Zhang et al. 2019). Hence, the soil moisture at shallow soil layer were larger than that of deep soil layer (Fig. 3).

Our findings highlighted that root-enhanced preferential flow is an important factor for SWC variation (Figs. 3–7). After dual-tracer experiments, soil moisture of the two sites increased by 70% compared with the ISWC. As compared with DF, the proportion rising was higher in CF (Figs. 4 and 5). The SWC distribution patterns for  $DC > 0$  and  $DC = 0$  sections were apparently different in 0–40 cm soil layer. In addition, the proportion of  $SWC_{DC} > 0$  larger than ISWC

**Table 3** Correlations coefficients of root traits and SWC

SWC (%)	Root traits		RSD (mm <sup>2</sup> /cm <sup>3</sup> )				RVD (mm <sup>3</sup> /cm <sup>3</sup> )				
	RA (number/dm <sup>2</sup> )	RLD (mm/cm <sup>3</sup> )	$d \leq 1$ mm		$1 < d \leq 2$ mm		$2 < d \leq 5$ mm		$d \leq 1$ mm		
			$d \leq 1$ mm	$1 < d \leq 2$ mm	$2 < d \leq 5$ mm	$d \leq 1$ mm	$1 < d \leq 2$ mm	$2 < d \leq 5$ mm	$d \leq 1$ mm	$1 < d \leq 2$ mm	
SWC <sub>large rainfall amount</sub>	0.905**	0.857**	0.690	0.595	0.929**	0.690	0.323	0.976**	0.643	0.643	0.310
SWC <sub>extreme rainfall amount</sub>	0.571	0.476	0.690	0.452	0.643	0.690	0.180	0.738*	0.738*	0.738*	0.167

SWC<sub>large rainfall amount</sub> SWC measured during large rainfall amount, SWC<sub>extreme rainfall amount</sub> SWC measured during extreme rainfall amount, RA root abundant, RLD root length density, RSD root surface density, RVD root volume density, d root diameter

\*  $P < 0.05$ ; \*\*  $P < 0.01$

was higher than the region of  $\text{SWC}_{\text{DC}} = 0$  (Fig. 5). These results might be related that the preferential flow path, which transmit more than 90% of the infiltration water and is the main site of water transport process during infiltration (Sanders et al. 2012). Another possible explanation for this result may be the differences of water-repellent effect between soil matrix and preferential flow path. After soil water infiltrates into soils, low water-repellent effect of soil matrix reduces soil water content, and moisture is absorbed by preferential flow path with large soil pores (Liu et al. 2021). Based on the previous study conducted in our study area, preferential flow path contained more roots than in soil matrix (Zhang et al. 2017). Large amounts of roots accumulated soil water and increased soil moisture of preferential flow paths (Ghestem et al. 2011).

This study found that the linkages between root traits and SWC were different at different diameter classes and different rainfall amounts (Table 3). For large rainfall amount, SWC had an extremely significant positive relationships with RA ( $d \leq 5$  mm), RLD ( $d \leq 1$  mm), RSD ( $d \leq 1$  mm), and RVD ( $d \leq 1$  mm) ( $P < 0.01$ ). Macropores generated by roots can act as preferential flow path for faster penetration (Guo et al. 2019a). Our finding is consistent with those reported by Johnson and Lehmann (2006) and Schwärzel et al. (2012). Meantime, root traits (RLD, RSD, and RVD) of  $d \leq 1$  mm was more closely related to SWC as compared with other diameter classes (Table 3). This result may be explained by lager amount, better connectivity, as well as greater root and soil contact area of finer roots. As regards to extreme rainfall amount, the correlations between SWC and root traits was weaker than that under larger rainfall amount (Table 3). Additionally, the coefficient between SWC and RSI (root-solute interaction) were larger under large rainfall amount than that under extreme rainfall amount in both sites (Fig. 7). These results can be explained by the study of Wang and Zhang (2011), who stated that the effect of macropores on soil water distribution was more evident under low infiltration amount (20–40 mm) as compared with large infiltration amount (60–80 mm).

The significant correlation between preferential flow indexes and SWC were shown in Fig. 6, indicating the response of SWC to root-enhanced preferential flow. Our results indicate that the higher degree of preferential flow and hydrological connectivity, the higher the SWC of soil profiles. These findings are consistent with previous studies (Mei et al. 2018; Schwen et al. 2014; Sheng et al. 2014; Wang and Zhang, 2011). RSI indicated the intensity of infiltration in the root zone. The larger RSI, the higher infiltration intensity in the root zone (Luo et al. 2019b). Statistically significant and relations were observed between RSI and SWC (Fig. 7). Our study matches previous observations which stated that roots can enhance the

preferential flow processes (Helliwell et al. 2017; Jiang et al. 2018; Schwärzel et al. 2012; Zhang et al. 2017). When the RSI was equal to 0, the SWC was larger than 0 (Fig. 7). It was possible that these results are due to other factors (rock fragments, soil texture, or cracks) that influence the SWC distribution. In this study, higher SWC was found when  $\text{RSI} > 0$  than for  $\text{RSI} = 0$ , which also is in accordance with our previous findings (Fig. 4–6). Our findings highlighted the importance of root-enhanced preferential flow in SWC redistribution for forest soils.

The three-dimensional root architecture characteristics is probably important for preferential flow and soil water redistribution. However, it was impossible to obtain this in our study. The root environment is complex and not directly observable. Further research should be undertaken to investigate the temporal and spatial response of soil water content to root-enhanced preferential flow by combining electrical resistivity tomography, penetrating radar, and CT tomography technologies (Guo et al. 2020; Hu et al. 2011, 2018) improve the understanding of effects of root-enhanced preferential flow on spatiotemporal variations of soil water redistribution.

## 5 Conclusion

The relations among roots, preferential flow, and soil moisture distribution were study in deciduous and coniferous forests. Our study demonstrated that soil water accumulated in the upper soil layer (0–20 cm) where roots were abundant as compared to deeper soil layers, which was more apparent in deciduous forest soils than in coniferous forest under different rainfall amounts. Compared with deciduous forest, coniferous forest with higher degree of preferential flow had larger soil moisture in soil profiles after rainfall amounts. In forest soils, soil sections with presence of preferential flow had higher soil water moisture than in the soil matrix. Compared with extreme rainfall amount, the effect of root traits on soil water distribution was more evident under large rainfall amount. Root-solute interaction was significantly and positively correlated with soil water content in the 0–40 cm soil layer. These findings provide direct evidence of the relations among soil water content, root traits, and preferential flow in forest soils. This study has shown that the different soil moisture redistribution features can be induced by root-enhanced preferential flow of different tree species, which will contribute to the management of water resources in forest soils, the understanding the eco-hydrological processes in forest ecosystem, and the modeling of the soil water flow in the unsaturated zone.

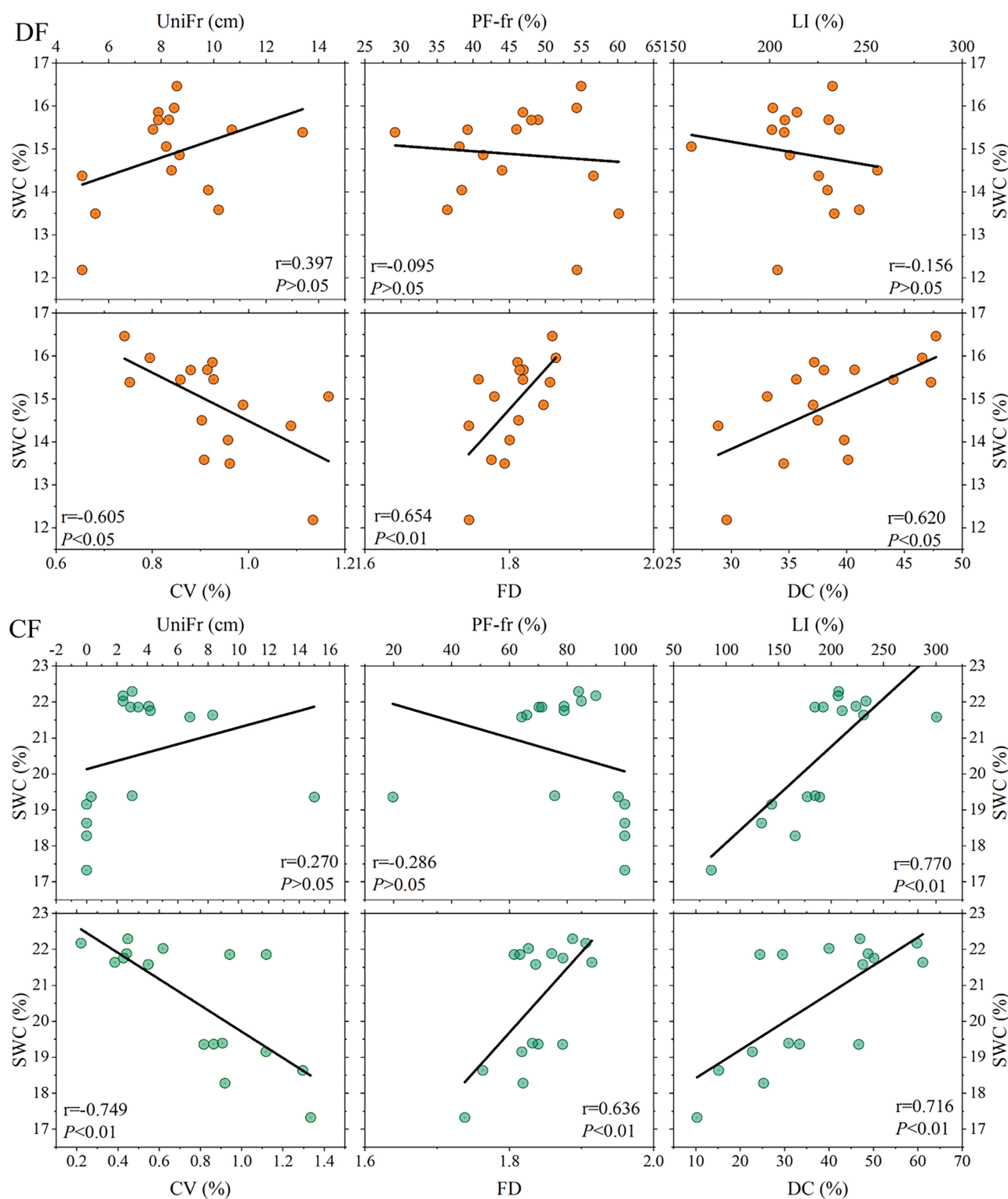


**Fig. 6** Relationships between preferential flow indices and SWC at DF and CF. DF, deciduous forest; CF, coniferous forest; UniFr, uniform percolation depth; PF-fr, preferential flow fraction; LI, length index; CV, coefficient of variation of DC; FD, fractal dimension; DC, dye coverage

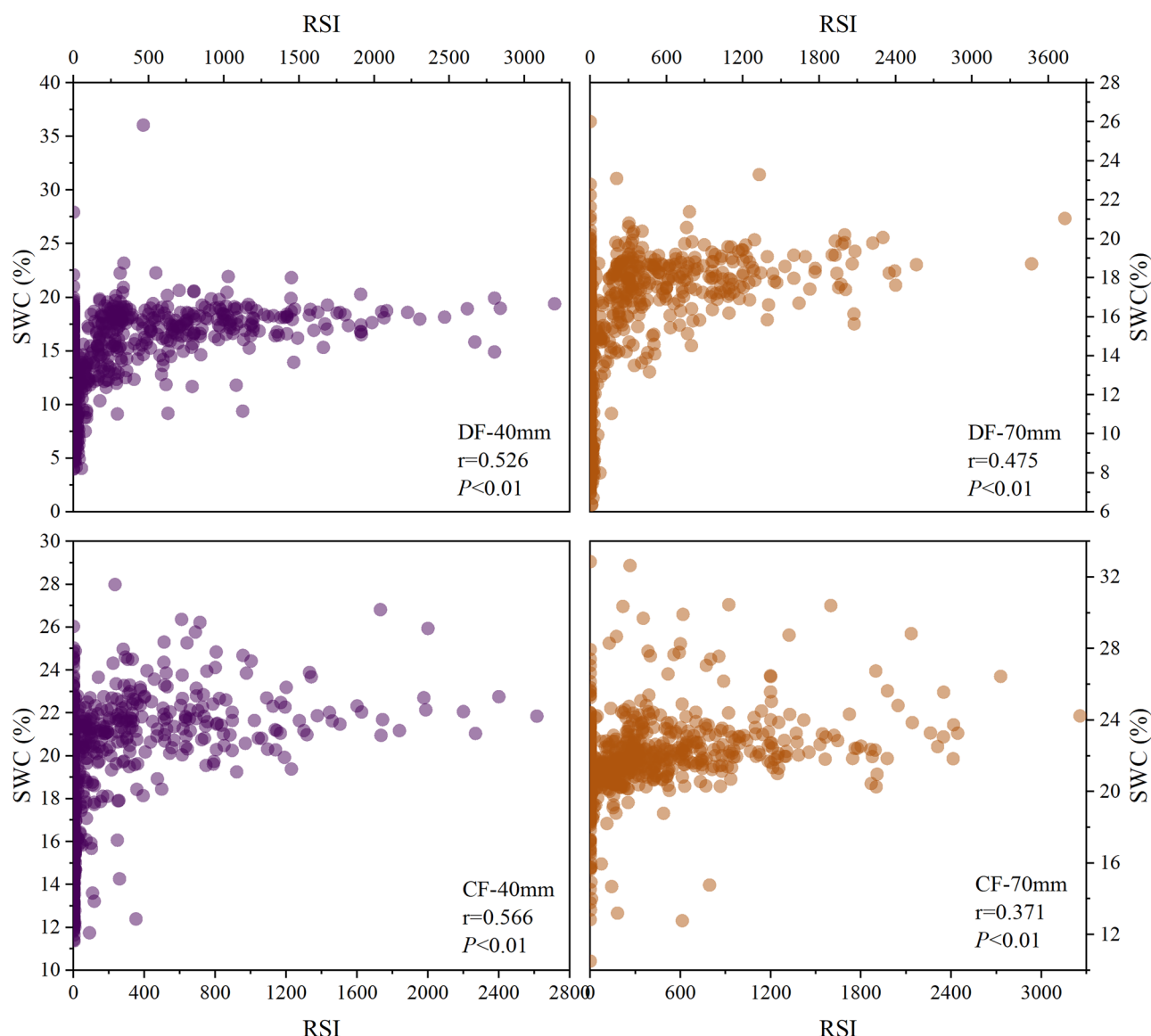


**Fig. 7** Relationships between SWC and RSI; DF and CF are deciduous and coniferous forests, respectively; DF-40 and CF-40 mm are for large rainfall amount (40 mm). DF-70 and CF-70 mm are for extreme

rainfall amount (70 mm); SWC, soil water content (%); RSI, root-solute interaction

**Author contribution** Ziteng Luo: conceptualization, methodology, investigation, data curation, formal analysis, visualization, writing – original draft, writing—review & editing, funding acquisition & project administration. Jianzhi Niu: conceptualization, methodology, investigation, data curation, writing – original draft, writing—review & editing, funding acquisition, & project administration. Shuqin He: conceptualization, methodology, visualization, writing – review & editing. Linus Zhang: investigation, writing – review & editing. Xiongwen Chen: investigation, writing – review & editing. Bo Tan: writing – review & editing. Di Wang: methodology. Ronny Berndtsson: conceptualization, writing – review & editing.

**Funding** This work was supported by the National Natural Science Foundation of China [Grant number 41877154]; the National Natural Science Foundation of China [Grant number 41741024]; the Natural Science Foundation of Sichuan Province [Grant number 2022NSFSC1037].

## Declarations

**Conflict of interest** The authors declare no competing interests.

## References

- Allaire SE, Roulier S, Cessna AJ (2009) Quantifying preferential flow in soils: a review of different techniques. *J Hydrol* 378(1–2):179–204. <https://doi.org/10.1016/j.jhydrol.2009.08.013>
- Backnäs S, Laine-Kaulio H, Kløve B (2012) Phosphorus forms and related soil chemistry in preferential flow paths and the soil matrix of a forested podzolic till soil profile. *Geoderma* 189–190:50–64. <https://doi.org/10.1016/j.geoderma.2012.04.016>

- Bak F, Nybroe O, Zheng B, Badawi N, Hao X, Nicolaisen MH, Aamand J (2019) Preferential flow paths shape the structure of bacterial communities in a clayey till depth profile. *FEMS Microbiol Ecol* 95(3). <https://doi.org/10.1093/femsec/fiz008>
- Bargués Tobella A, Reese H, Almaw A, Bayala J, Malmer A, Ilstedt LH, U (2014) The effect of trees on preferential flow and soil infiltrability in an agroforestry parkland in semiarid Burkina Faso. *Water Resour Res* 50:3342–3354. <https://doi.org/10.1002/2013WR015197>
- Beven K, Germann P (2013) Macropores and water flow in soils revisited. *Water Resour Res* 49:3071–3092. <https://doi.org/10.1002/wrcr.20156>
- Cui Z, Wu G, Huang Z, Liu Y (2019) Fine roots determine soil infiltration potential than soil water content in semi-arid grassland soils. *J Hydrol* 578:124023. <https://doi.org/10.1016/j.jhydrol.2019.124023>
- Dai L, Zhang Y, Liu Y, Xie L, Zhao S, Zhang Z, Lv X (2020) Assessing hydrological connectivity of wetlands by dye-tracing experiment. *Ecol Indic* 119:106840. <https://doi.org/10.1016/j.ecolind.2020.106840>
- de Lima RP, Rolim MM, Toledo MPS, Tormena CA, Da Silva AR, Silva E, IAC, Pedrosa EMR (2022) Texture and degree of compactness effect on the pore size distribution in weathered tropical soils. *Soil till Res* 215:105215. <https://doi.org/10.1016/j.still.2021.105215>
- Dusek J, Vogel T, Lichner L, Čipáková A, Dohnal M (2006) Simulated cadmium transport in macroporous soil during heavy rainstorm using dual-permeability approach. *Biologia* 61:S251–S254. <https://doi.org/10.2478/s11756-006-0167-9>
- Dubus IG, Brown CD (2002) Sensitivity and first-step uncertainty analyses for the preferential flow model MACRO. *J Environ Qual* 31:227–240. <https://doi.org/10.2134/jeq2002.2270>
- Franklin SM, Kravchenko AN, Vargas R, Vasilas B, Fuhrmann JJ, Jin Y (2021) The unexplored role of preferential flow in soil carbon dynamics. *Soil Biol Biochem* 161:108398. <https://doi.org/10.1016/j.soilbio.2021.108398>
- Gao Z, Hu X, Li X (2021) Changes in soil water retention and content during shrub encroachment process in Inner Mongolia, northern China. *Catena* 206:105528. <https://doi.org/10.1016/j.catena.2021.105528>
- Ghestem M, Sidle RC, Stokes A (2011) The influence of plant root systems on subsurface flow: implications for slope stability. *Bioscience* 61(11):869–879. <https://doi.org/10.1525/bio.2011.61.11.6>
- Guo L, Liu Y, Wu G, Huang Z, Cui Z, Cheng Z, Zhang R, Tian F, He H (2019a) Preferential water flow: Influence of alfalfa (*Medicago sativa* L.) decayed root channels on soil water infiltration. *J Hydrol* 578:124019. <https://doi.org/10.1016/j.jhydrol.2019.124019>
- Guo L, Lin H, Fan B, Nyquist J, Toran L, Mount GJ (2019b) Preferential flow through shallow fractured bedrock and a 3D fill-and-spill model of hillslope subsurface hydrology. *J Hydrol* 576:430–442. <https://doi.org/10.1016/j.jhydrol.2019.06.070>
- Guo L, Mount GJ, Hudson S, Lin H, Levia D (2020) Pairing geophysical techniques improves understanding of the near-surface critical zone visualization of preferential routing of stemflow along coarse roots. *Geoderma* 357:113953. <https://doi.org/10.1016/j.geoderma.2019.113953>
- Hendrickx JMH, Flury M (2001) Uniform and preferential flow mechanisms in the vadose zone. Conceptual Models of Flow and Transport in the Fractured Vadose Zone. National Academy Press, Washington, DC, National Research Council, pp 149–187
- Helliwell JR, Sturrock CJ, Mairhofer S, Craigon J, Ashton RW, Miller AJ, Whalley WR, Mooney SJ (2017) The emergent rhizosphere: imaging the development of the porous architecture at the root-soil interface. *Sci Rep-UK* 7:14875–14910. <https://doi.org/10.1038/s41598-017-14904-w>
- Hu W, Shao MG, Han FP, Reichardt K (2011) Spatio-temporal variability behavior of land surface soil water content in shrub- and grass-land. *Geoderma* 162(3–4):260–272. <https://doi.org/10.1016/j.geoderma.2011.02.008>
- Hu X, Li X, Guo L, Liu Y, Wang P, Zhao Y, Cheng Y, Lyn Y, Liu L (2018) Influence of shrub roots on soil macropores using X-ray computed tomography in a shrub-encroached grassland in Northern China. *J Soil Sediment* 19(8):1970–1980. <https://doi.org/10.1007/s11368-018-2218-6>
- Huang Z, Tianm F, Wu G, Liu Y, Dang Z (2016) Legume grasslands promote precipitation infiltration better than gramineous grasslands in arid regions. *Land Degrad Dev* 28(1):309–316. <https://doi.org/10.1002/ldr.2635>
- Huang Z, Sun L, Liu Y, Liu YF, López-Vicente M, Wei X, Wu G (2019) Alfalfa planting significantly improved alpine soil water infiltrability in the Qinghai-Tibetan Plateau. *Agr Ecosyst Environ* 285:106606. <https://doi.org/10.1016/j.agee.2019.106606>
- Jiang X, Liu X, Wang E, Li X, Sun R, Shi W (2015) Effects of tillage pan on soil water distribution in alfalfa-corn crop rotation systems using a dye tracer and geostatistical methods. *Soil till Res* 150:68–77. <https://doi.org/10.1016/j.still.2015.01.009>
- Jiang X, Liu W, Chen C, Liu J, Yuan Z, Jin B, Yu X (2018) Effects of three morphometric features of roots on soil water flow behavior in three sites in China. *Geoderma* 320:161–171. <https://doi.org/10.1016/j.geoderma.2018.01.035>
- Johnson MS, Lehmann J (2006) Double-funneling of trees: Stemflow and root-induced preferential flow. *Écoscience* 13(3):324–333. <https://doi.org/10.2980/i1195-6860-13-3-324.1>
- Jørgensen PR, Hoffmann M, Kistrup JP, Bryde C, Bossi R, Villholth KG (2002) Preferential flow and pesticide transport in a clay-rich till: field, laboratory, and modeling analysis. *Water Resour Res* 38(11):28–1–28–15. <https://doi.org/10.1029/2001WR000494>
- Keesstra S, Pereira P, Novara A, Brevik EC, Azorin-Molina C, Parras-Alcantara L, Jordan A, Cerda A (2016) Effects of soil management techniques on soil water erosion in apricot orchards. *Sci Total Environ* 551–552:357–366. <https://doi.org/10.1016/j.scitotenv.2016.01.182>
- Laine-Kaulio H, Backnäs S, Koivusalo H, Laurén A (2015) Dye tracer visualization of flow patterns and pathways in glacial sandy till at a boreal forest hillslope. *Geoderma* 259–260:23–34. <https://doi.org/10.1016/j.geoderma.2015.05.004>
- Legout A, Legout C, Nys C, Dambrine E (2009) Preferential flow and slow convective chloride transport through the soil of a forested landscape (Fougères, France). *Geoderma* 151(3–4):179–190. <https://doi.org/10.1016/j.geoderma.2009.04.002>
- Lepore BJ, Morgan C, Norman JM, Molling CC (2009) A mesopore and matrix infiltration model based on soil structure. *Geoderma* 152(3–4):301–313. <https://doi.org/10.1016/j.geoderma.2009.06.016>
- Liu H, Lin H (2015) Frequency and control of subsurface preferential flow: from pedon to catchment scales. *Soil Sci Soc Am J* 79(2):362–377. <https://doi.org/10.2136/sssaj2014.08.0330>
- Liu Y, Cui Z, Huang Z, López-Vicente M, Wu G (2019a) Influence of soil moisture and plant roots on the soil infiltration capacity at different stages in arid grasslands of China. *Catena* 182:104147. <https://doi.org/10.1016/j.catena.2019.104147>
- Liu Y, Zhang Y, Xie L, Zhao S, Dai L, Zhang Z (2021) Effect of soil characteristics on preferential flow of *Phragmites australis* community in Yellow River delta. *Ecol Indic* 125:107486. <https://doi.org/10.1016/j.ecolind.2021.107486>
- Liu Y, Guo L, Huang Z, López-Vicente M, Wu G (2020) Root morphological characteristics and soil water infiltration capacity in semi-arid artificial grassland soils. *Agr Water Manage* 235:106153. <https://doi.org/10.1016/j.agwat.2020.106153>
- Liu Z, Yu X, Jia G, Jia J, Lou Y, Lu W (2017) Contrasting water sources of evergreen and deciduous tree species in rocky mountain area

- of Beijing, China. *Catena* 150:108–115. <https://doi.org/10.1016/j.catena.2016.11.013>
- Liu Z, Yu X, Jia G (2019b) Water uptake by coniferous and broad-leaved forest in a rocky mountainous area of northern China. *Agr Forest Meteorol* 265:381–389. <https://doi.org/10.1016/j.agrmet.2018.11.036>
- Luo Z, Niu J, Zhang L, Chen X, Zhang W, Xie B, Du J, Zhu Z, Wu S, Li X (2019a) Roots-enhanced preferential flows in deciduous and coniferous forest soils revealed by dual-tracer experiments. *J Environ Qual* 48(1):136–146. <https://doi.org/10.2134/jeq2018.03.0091>
- Luo Z, Niu J, Xie B, Zhang L, Chen X, Berndtsson R, Du J, Ao J, Yang L, Zhu S (2019b) Influence of root distribution on preferential flow in deciduous and coniferous forest soils. *Forests* 10(11):986. <https://doi.org/10.3390/f10110986>
- Mei X, Zhu Q, Ma L, Zhang D, Wang Y, Hao W (2018) Effect of stand origin and slope position on infiltration pattern and preferential flow on a Loess hillslope. *Land Degrad Dev* 29:1353–1365. <https://doi.org/10.1002/lrd.2928>
- Meng C, Niu J, Li X, Luo Z, Du X, D J, Lin X, Yu X (2017) Quantifying soil macropore networks in different forest communities using industrial computed tomography in a mountainous area of North China. *J Soil Sediment* 17(9):2357–2370. <https://doi.org/10.1007/s11368-016-1441-2>
- Ni J, Luo D, Xia J, Zhang Z, Hu G (2015) Vegetation in karst terrain of southwestern China allocates more biomass to roots. *Solid Earth* 6:799–810. <https://doi.org/10.5194/se-6-799-2015>
- Porporato A, D'odorico P, Laio F, Ridolfi L, Rodriguez-Iturbe I (2002) Ecohydrology of water-controlled ecosystems. *Adv Water Resour* 25:1335–1348. [https://doi.org/10.1016/S0309-1708\(02\)00058-1](https://doi.org/10.1016/S0309-1708(02)00058-1)
- Raijada A, Jayaprakash J, Rathore AC, Tomar JMS (2013) Distribution of fine root biomass of fruit and forest tree species raised on old river bed lands in the north west Himalaya. *Trop Ecol* 54(2):251–261
- Revelli R, Ridolfi L (2003) Transport of reactive chemicals in sediment-laden streams. *Adv Water Resour* 26(8):815–831. [https://doi.org/10.1016/S0309-1708\(03\)00077-0](https://doi.org/10.1016/S0309-1708(03)00077-0)
- Rodríguez F, Mayor AG, Rietkerk M, Bautista S (2018) A null model for assessing the cover-independent role of bare soil connectivity as indicator of dryland functioning and dynamics. *Ecol Indicat* 94:512–519. <https://doi.org/10.1016/j.ecolind.2017.10.023>
- Sanders EC, Najm MA, Mohtar R, Kladivko E, Schulze D (2012) Field method for separating the contribution of surface-connected preferential flow pathways from flow through the soil matrix. *Water Resour Res* 48(4):W04534. <https://doi.org/10.1029/2011WR011103>
- Schwärzel K, Ebermann S, Schalling N (2012) Evidence of double-funneling effect of beech trees by visualization of flow pathways using dye tracer. *J Hydrol* 470–471:184–192. <https://doi.org/10.1016/j.jhydrol.2012.08.048>
- Schwen A, Backus J, Yang Y, Wendroth O (2014) Characterizing land use impact on multi-tracer displacement and soil structure. *J Hydrol* 519:1752–1768. <https://doi.org/10.1016/j.jhydrol.2014.09.028>
- Sheng F, Liu H, Wang K, Zhang R, Tang Z (2014) Investigation into preferential flow in natural unsaturated soils with field multiple-tracer infiltration experiments and the active region model. *J Hydrol* 508:137–146. <https://doi.org/10.1016/j.jhydrol.2013.10.048>
- Tecon R, Or D (2016) Bacterial flagellar motility on hydrated rough surfaces controlled by aqueous film thickness and connectedness. *Sci Rep-UK* 6(1):19409. <https://doi.org/10.1038/srep19409>
- Wang F, Wang G, Cui J, Guo L, Mello CR, Boyer EW, Tang X, Yang Y (2022) Preferential flow patterns in forested hillslopes of the east Tibetan Plateau revealed by dye tracing and soil moisture network. *Eur J Soil Sci* 74(4):e13294. <https://doi.org/10.1111/ejss.13294>
- Wang K, Zhang R (2011) Heterogeneous soil water flow and macropores described with combined tracers of dye and iodine. *J Hydrol* 397(1–2):105–117. <https://doi.org/10.1016/j.jhydrol.2010.11.037>
- Wu G, Liu Y, Yang Z, Cui Z, Deng L, Chang X, Shi Z (2017) Root channels to indicate the increase in soil matrix water infiltration capacity of arid reclaimed mine soils. *J Hydrol* 546:133–139. <https://doi.org/10.1016/j.jhydrol.2016.12.047>
- Wu G, Cui Z, Huang Z (2021) Contribution of root decay process on soil infiltration capacity and soil water replenishment of planted forestland in semi-arid regions. *Geoderma* 404:115289. <https://doi.org/10.1016/j.geoderma.2021.115289>
- Wu Q, Zhang J, Lin W, Wang G (2014) Applying dyeing tracer to investigate patterns of soil water flow and quantify preferential flow in soil columns. *Transactions of the Chin Soc of Agr Eng* 30(7):82–90. <https://doi.org/10.3969/j.issn.1002-6819.2014.07.010>
- Yan J, Zhao W (2016) Characteristics of preferential flow during simulated rainfall events in an arid region of China. *Environ Earth Sci* 75:566. <https://doi.org/10.1007/s12665-015-5101-4>
- Young IM, Bengough AG (2018) The search for the meaning of life in soil: an opinion. *Eur J Soil Sci* 69:31–38. <https://doi.org/10.1111/ejss.12514>
- Zhang J, Lei T, Qu L, Zhang M, Chen P, Gao X, Chen C, Yuan L (2019) Method to quantitatively partition the temporal preferential flow and matrix infiltration in forest soil. *Geoderma* 347:150–159. <https://doi.org/10.1016/j.geoderma.2019.03.026>
- Zhang Y, Niu J, Zhang M, Xiao Z, Zhu W (2017) Interaction Between Plant Roots and Soil Water Flow in Response to Preferential Flow Paths in Northern China. *Land Degrad Dev* 28(2):648–663. <https://doi.org/10.1002/lrd.2592>
- Zhang ZB, Peng X, Zhou H, Lin H, Sun H (2015) Characterizing preferential flow in cracked paddy soils using computed tomography and breakthrough curve[J]. *Soil till Res* 146:53–65. <https://doi.org/10.1016/j.still.2014.05.016>
- Zhu X, Chen C, Wu J, Yang J, Zhang W, Zou X, Liu W, Jiang X (2019) Can intercrops improve soil water infiltrability and preferential flow in rubber-based agroforestry system? *Soil Soil till Res* 191:327–339. <https://doi.org/10.1016/j.still.2019.04.017>
- Zuo F, Li X, Yang X, Ma Y, Shi F, Liao Q, Li D, Wang Y, Wang R (2021) Linking root traits and soil moisture redistribution under *Achnatherum splendens* using electrical resistivity tomography and dye experiments. *Geoderma* 386:114908. <https://doi.org/10.1016/j.geoderma.2020.114908>

**Publisher's Note** Springer Nature remains neutral with regard to jurisdictional claims in published maps and institutional affiliations.

Springer Nature or its licensor (e.g. a society or other partner) holds exclusive rights to this article under a publishing agreement with the author(s) or other rightsholder(s); author self-archiving of the accepted manuscript version of this article is solely governed by the terms of such publishing agreement and applicable law.